energy&fuels

Article

pubs.acs.org/EF

Modeling Reservoir Connectivity and Tar Mat Using Gravity-Induced Asphaltene Compositional Grading

Sai R. Panuganti,[†] Francisco M. Vargas,[‡] and Walter G. Chapman*[,†]

[†]Department of Chemical and Biomolecular Engineering, Rice University, Houston, Texas 77005, United States

[‡]Department of Chemical Engineering, The Petroleum Institute, Abu Dhabi, United Arab Emirates

ABSTRACT: Reservoir compartmentalization is one of the major issues on both on- and offshore reservoirs. High capital costs are involved especially in deepwater exploration and production, making it essential to assess prior to production the extent of compartmentalization within a reservoir. Within a continuous reservoir, fluid properties vary with depth because of compositional grading. Considerable fluid flow is required to attain thermodynamic equilibrium yielding compositional gradients, suggesting connectivity. In this work, an algorithm that makes use of the perturbed-chain statistical associating fluid theory (PC-SAFT) equation of state (EoS) is proposed to address the isothermal asphaltene compositional grading in a uniform gravitational field. The model is validated against well log and production data. The results are compared to field data to evaluate the reservoir compartmentalization. An approximate analytical solution for asphaltene compositional grading, derived from solution thermodynamics, is also presented. Asphaltene compositional grading under extreme cases can lead to tar-mat formation. The PC-SAFT asphaltene compositional grading introduced in this study is extended to model the possibility of a tar-mat formation because of gravitational segregation of asphaltene.

1. INTRODUCTION

Asphaltene are defined as the fraction of a crude oil that dissolves in toluene and is insoluble in *n*-heptane or *n*-pentane. Modeling asphaltene thermodynamic behavior has a potential application in understanding reservoir connectivity. Compartmentalization arising because of different factors, such as impermeable layers and faults, leads to the lack of reservoir connectivity. This work proposes a combined solution to the individually ill-posed problems of reservoir compartmentalization and tar-mat occurrence. Tar mat predominantly represents a non-producible oil in place and low-permeability intra-reservoir flow barrier.

Compartmentalization is one of the major problems in both on- and offshore reservoirs. It makes recovery more difficult because of poor drainage for a given number of wells. High capital costs are involved, especially in deepwater, making it essential to assess prior to production the extent of compartmentalization within a reservoir. Seismic data and discontinuous variation of fluid properties (e.g., chemistry, density, and viscosity) are commonly used in an attempt to assess the level of compartmentalization. The varying fluid properties along the depth of a reservoir are due to compositional grading.[1] In oil columns, considerable fluid flow is required to reach thermodynamic equilibrium, yielding such compositional gradients, and, thus, suggests reservoir connectivity better than pressure communication where little fluid flow is required.[2] In particular, reservoir connectivity can be best understood on the basis of continuous characteristics of the asphaltene compositional gradient, because to equilibrate asphaltene, the heaviest component of crude oil with by far the least mobility necessitates substantial permeability.[3]

The continuous variations in the gas/oil ratio (GOR) and composition have been reported by industries for continuous reservoirs through significant ranges in depth.[4] The continuous variation is accounted for thermodynamic equilibrium and, thus, connectivity of a reservoir.[5] In general, there is a greater GOR during production from the upper parts of a formation. The analysis by Hoier and Whitson[6] accounts for the GOR and composition of equilibrium fluids as measured by the downhole fluid analysis (DFA). DFA also measures crude oil optical density (OD) using infrared light. This OD is directly proportional to the asphaltene content.[7] However, Whitson or others did not analyze compositional grading related to asphaltene because of limited knowledge of asphaltene prior to 2000. In this work, an algorithm that makes use of the perturbed-chain statistical associating fluid theory (PC-SAFT) equation of state (EoS) is proposed to address the isothermal asphaltene compositional grading. The crude oils A and B studied here are characterized at downhole conditions using the PC-SAFT characterization methodology developed by Rice University and The Petroleum Institute. In their PC-SAFT characterization paper, it was showed that parameters estimated at a particular operating condition work well to predict the liquid−liquid/vapor equilibrium at other operating conditions, including a change of system composition.[8]

PC-SAFT EoS, which has been successfully applied for asphaltene precipitation in flow assurance, is for the first time extended to model asphaltene distribution in oil columns. In the present work, the possible changes in asphaltene composition with depth, which could result from the attainment of thermodynamic equilibrium in a uniform gravitational field, are modeled by PC-SAFT and compared

Special Issue: 12th InternationalConference on Petroleum Phase Behaviorand Fouling

Received: August 24, 2011
Revised: November 24, 2011
Published: November 28, 2011

 © 2011 American Chemical Society dx.doi.org/10.1021/ef201280d | *Energy Fuels* 2012, 26, 2548−2557

to field data to evaluate the reservoir compartmentalization. On the basis of solution thermodynamics, an approximate analytical solution for predicting the asphaltene compositional gradient is also presented. The analytical solution will be helpful for sensitivity analysis and approximate estimate of the asphaltene compositional gradient.

The asphaltene compositional gradient can lead to significant variations in crude oil viscosity,[9] and extreme cases of asphaltene compositional grading can lead to tar-mat formation.[10] Many of the Middle East oil fields are rimmed by large and thick accumulation of highly viscous extra heavy oil.[11] It is termed as tar mat and represents a reservoir zone containing highly enriched asphaltene (20−60 wt %) relative to the oil column.[12] Tar mat is an important organic barrier for an oil reservoir and must be modeled as accurately as possible to obtain a reliable simulation model and, ultimately, predictive production profiles. The PC-SAFT asphaltene compositional grading introduced in this study is extended to model the possibility of a tar-mat formation because of gravitational segregation of asphaltene.

2. PC-SAFT CHARACTERIZATION OF CRUDE OIL AT DOWNHOLE CONDITIONS

This section provides a brief methodology of the PC-SAFT characterization of crude oil at downhole conditions. A detailed description of the procedure is provided elsewhere.[13] The association term in SAFT can be neglected in the asphaltene modeling work, because it is the polarizability and not the polarity of asphaltene molecules that dominate their phase behavior.[14] Therefore, the PC-SAFT EoS requires just three temperature-independent parameters: the diameter of each molecular segment (σ), the number of segments per molecule (m), and the segment−segment dispersion energy (ε/k) for each non-associating component.

In the characterization procedure for the live oil, the gas phase consists of six pseudo-components: nitrogen (N_2), carbon dioxide (CO_2), methane (CH_4), ethane (C_2H_6), propane (C_3H_8), and heavy gas pseudo-component (hydrocarbons C_4 and heavier). The characterization is based on the compositional information for the gas phase. The PC-SAFT EoS parameters for the pure components, N_2, CO_2, and C_1−C_3, are available in the literature.[15] The average molecular weight of the heavy gas pseudo-component (mostly consisting of saturates) is used to estimate the corresponding PC-SAFT parameters through correlations developed by Gonzalez et al.[16]

The liquid phase is represented by three pseudo-components: saturates, aromatics plus resins (A + R), and asphaltenes. The characterization of this phase is based on the stock tank oil (STO) compositional information and saturates, aromatics, resins, and asphaltenes (SARA) analysis. All asphaltenes are found in the heaviest subfraction. Above the C_9 cut, the proportion of saturates and asphaltenes are defined such that total saturates, A + R, and asphaltenes match the content reported by SARA analysis.

The PC-SAFT parameters for saturates and aromatic plus resin pseudo-components are calculated from their average molecular weight,[16] and the correlations are provided in Table 1. The aromatic plus resin pseudo-components are linearly weighted by the aromaticity parameter (γ), which determines the A + R tendency to behave as polynuclear aromatic (PNA) ($\gamma = 1$) or benzene derivative ($\gamma = 0$).[16] The aromaticity is tuned for the fluid to meet the values of density and bubble point simultaneously. Increasing aromaticity increases the density because of the increased PNA content. At the same time, bubble pressure also increases because the lighter components in the oil now have a lower affinity to stay in the liquid phase. In the current work, a good estimate of the system density is more important than exactly matching the bubble pressure when predicting tar mat.

Asphaltene is treated as a monodisperse pseudo-component to minimize the number of parameters and at the same time capture the overall behavior. The PC-SAFT EoS parameters for a monodisperse asphaltene are estimated to precipitation onset measurements based on ambient titrations and/or depressurization measurements. Because of high polarizability, asphaltene exists as a pre-aggregated molecule even in good solvents, such as toluene.[17] The average molecular weight (MW) of such a pre-aggregated asphaltene is considered as 1700 g/mol.[18−20] Research on incorporating the polydispersity of asphaltene using PC-SAFT is currently underway at The Petroleum Institute, United Arab Emirates. The crude oils A and B from the two fields considered here behave differently. The oil properties are summarized in Table 2.

Table 1. PC-SAFT Correlations for Saturates and Aromatics Plus Resins[16]

correlation for saturates	aromatic + resin pseudo-components (γ is aromaticity) parameter = $(1-\gamma)$(benzene derivatives correlation) + γ(PNA correlation)
$m = (0.0257MW) + 0.8444$	$m = (1-\gamma)(0.0223MW + 0.751) + \gamma(0.0101MW + 1.7296)$
$\sigma(A) = 4.047 - ((4.8013 \ln(MW))/MW)$	$\sigma(A) = (1-\gamma)(4.1377 - (38.1483/MW)) + \gamma(4.6169 - (93.98/MW))$
$\ln(\varepsilon/k) = 5.5769 - (9.523/MW)$, K	$\varepsilon/k = (1-\gamma)(0.00436MW + 283.93) + \gamma(508 - (234100/(MW)^{1.5}))$, K

Table 2. Properties of Crude Oils A and B

	crude A	crude B
origin	Tahiti field	S field
GOR (scf/stb)	510	787
MW of reservoir fluid (g/mol)	131.5	97.75
MW of flashed gas (g/mol)	25.83	29.06
MW of STO (g/mol)	243.26	192.99
STO density (g/cm^3)	0.88	0.82
saturates (wt %)	52.90	66.26
aromatics (wt %)	29.70	25.59
resins (wt %)	13.20	5.35
asphaltenes (wt %)	4.00	2.80

2.1. Case I: Medium Oil (A) from the Tahiti Field. The crude oil A considered is from the Tahiti field in the Gulf of Mexico. The field has a GOR of ∼500 standard cubic feet per stock tank barrel (scf/stb), and the oil is medium with an American Petroleum Institute (API) gravity of ∼30°.

Asphaltene onset measurements at reservoir conditions were performed using the near-infrared (NIR) technique by Schlumberger, and the data were provided by Chevron. A detailed description of the experimental technique is elsewhere.[21] Key points are summarized here. A fixed wavelength in the infrared region is used to measure the asphaltene onset pressure (AOP) for a system temperature of 140 °F on STO with C_1, C_2, and C_3 as precipitants. A sub-sample from the cylinder is charged to the solid detection system and stabilized at the measurement temperature. Subsequently, the fluid is depressurized from a high pressure to below the bubble point in discrete steps. At each step, the fluid is stabilized for a couple of minutes. During the depressurization, the NIR light transmittance through the reservoir fluid is recorded as a function of the pressure and plotted in Figure 1. Deviation from the increasing light intensity trend represents the onset of asphaltene, and a decreasing trend implies clustering of these precipitated asphaltenes to block the transmitted light.

The characterized crude oil A with the PC-SAFT parameters is shown in Table 3. The modeled asphaltene phase envelope on a pressure−composition plot at a constant temperature of 140 °F is shown in Figure 2. From the successful agreement of experimental data with a constant set of parameters, asphaltenes from a particular sampled depth are now successfully characterized as one of the crude oil components. The inability to match the experimental AOP for C_3 titration is because of a non-expected trend of C_2 and C_3 amounts and onset pressure overlapping and is accounted for experimental error.

dx.doi.org/10.1021/ef201280d | Energy Fuels 2012, 26, 2548−2557

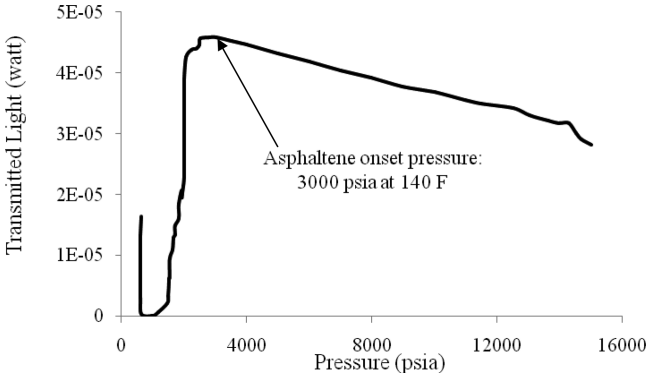

Figure 1. Crude A STO with C_2 asphaltene onset measurement using NIR light transmittance at 140 °F.[22]

Table 3. PC-SAFT Characterized Crude Oil A from the Tahiti Field

component	MW (g/mol)	mol %	m	σ (A)	ε/k (K)
N_2	28.01	0.03	1.20	3.31	90.96
CO_2	44.01	0.08	2.07	2.78	169.21
C_1	16.04	36.06	1.00	3.70	150.03
C_2	30.07	4.42	1.61	3.52	191.42
C_3	44.10	4.96	2.00	3.62	208.11
heavy gas	67.13	5.84	2.57	3.75	229.32
saturates	207.77	30.14	6.18	3.92	252.44
aromatics + resins (γ = 0.3)	280.20	18.19	6.27	4.09	337.00
asphaltenes	1700	0.28	39.00	4.28	349.00

2.2. Case II: Light Oil (B) from the S Field. In the second case, the crude oil B from the S field is considered. S is an onshore field with GOR of ~800 scf/stb. The oil is light with an API gravity of ~40° and a lower asphaltene content than crude A. As described in medium oil, the asphaltene onset measurements were performed using the NIR technique by Schlumberger, and the data were provided by Abu Dhabi Company for Onshore Oil Operations (ADCO). The NIR sample was live oil, and the onset is determined by depressurization at different temperatures. Crude B from the S field is characterized using the PC-SAFT characterization method, and the EoS parameters are estimated on the basis of experimental data of saturation and asphaltene onset pressures. The characterized crude oil B with the PC-SAFT parameters is shown in Table 4, and the phase envelope is plotted in Figure 3. The constant set of temperature-independent PC-SAFT binary interaction parameters used for both of the oils is shown in Table 5.[13] However, the K_{ij} between ethane and asphaltene for crude A was 0.08 to match the asphaltene precipitation onset when C_2 is added as the precipitant to crude A STO.

Table 4. PC-SAFT Characterized Crude Oil B

component	MW (g/mol)	mol %	PC-SAFT parameters m	σ (A)	ε/k (K)
N_2	28.04	0.17	1.21	3.31	90.96
CO_2	44.01	1.95	2.07	2.78	169.21
C_1	16.04	33.6	1.00	3.70	150.03
C_2	30.07	7.56	1.61	3.52	191.42
C_3	44.10	6.74	2.00	3.62	208.11
heavy gas	65.49	8.2	2.53	3.74	228.51
saturates	167.68	31.74	5.15	3.90	249.69
aromatics + resins (γ = 0.0)	253.79	9.91	6.41	3.99	285.00
asphaltenes	1700	0.13	33.00	4.20	353.50

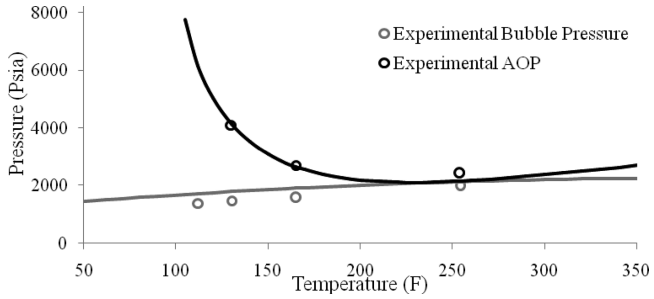

Figure 3. Asphaltene phase envelope for crude oil B generated by PC-SAFT (black line, asphaltene onset pressure; gray line, bubble pressure; and circles, experimental data).

3. ISOTHERMAL COMPOSITIONAL GRADING ALGORITHM

Gibbs was the first to derive the general conditions of equilibrium for a mixture of any number of fluids, but he

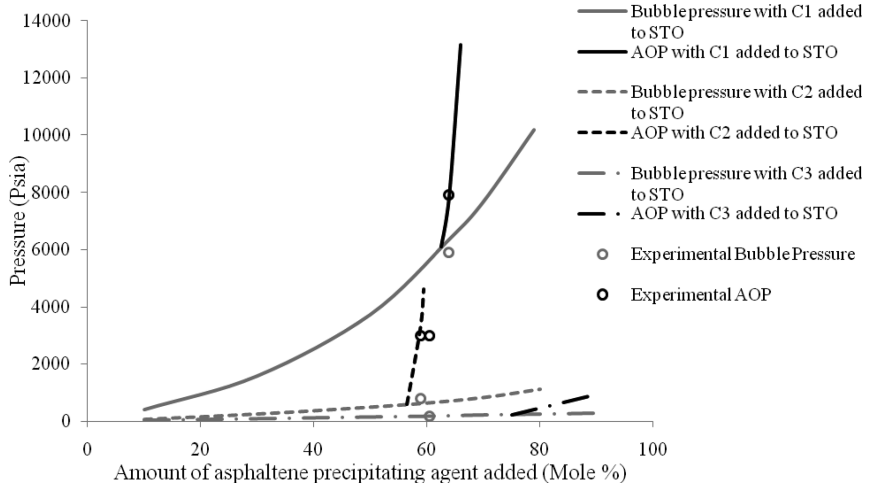

Figure 2. Asphaltene phase envelope curves for crude A STO with C_1, C_2, and C_3 precipitants at a constant system temperature of 140 °F (black line, AOP; gray line, bubble pressure; and circles, experimental data).

dx.doi.org/10.1021/ef201280d | Energy Fuels 2012, 26, 2548–2557

Table 5. PC-SAFT Temperature-Independent Binary Interaction Parameters (K_{ij}) for Crude Oil[13]

component	N_2	CO_2	H_2S	C_1	C_2	C_3	heavy gas	saturates	aromatics + resins	asphaltenes
N_2	0	0	0.09	0.03	0.04	0.06	0.075	0.14	0.158	0.16
CO_2		0	0.0678	0.05	0.097	0.1	0.12	0.13	0.1	0.1
H_2S			0	0.062	0.058	0.053	0.07	0.09	0.015	0.015
C_1				0	0	0	0.03	0.03	0.029	0.07
C_2					0	0	0.02	0.012	0.025	0.06
C_3						0	0.015	0.01	0.01	0.01
heavy gas							0	0.005	0.012	0.01
saturates								0	0.007	−0.004
aromatics + resins									0	0
asphaltenes										0

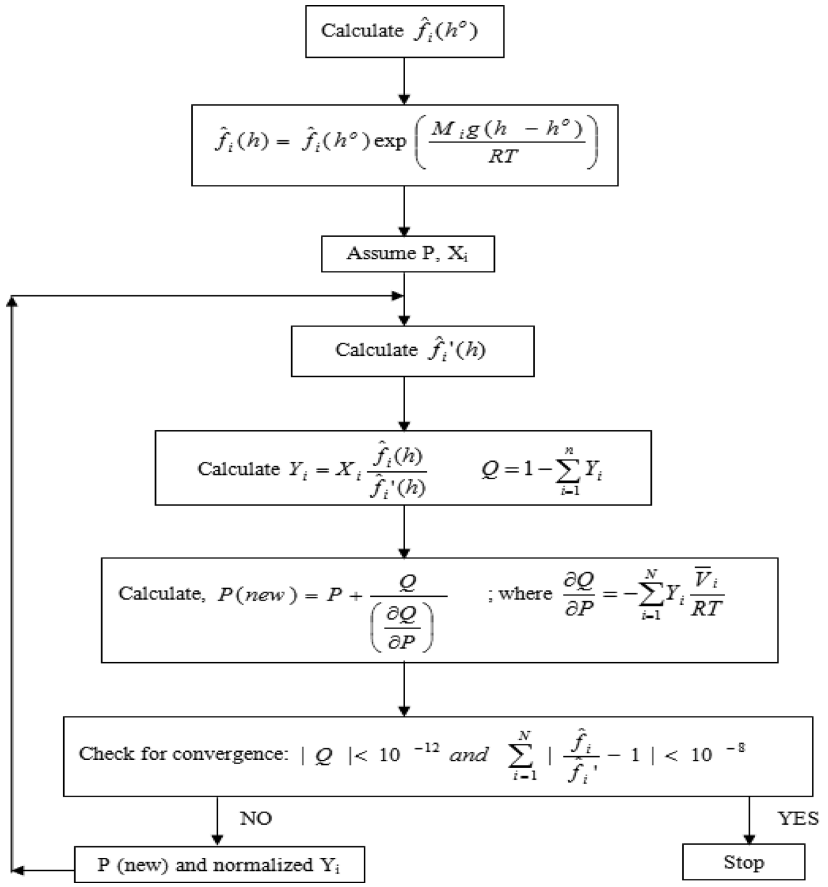

Figure 4. Flowchart of the isothermal gravitational compositional grading algorithm.

applied them only to ideal gas mixtures.[23] Gouy and Chaperon in 1887,[24] Duhem in 1888,[25] and van der Waals in 1900[26] considered binary mixtures but did not present explicit formulas for the results. Between 1930 and 1940, Muskat[27] and Sage and Lacey[28] formulated equations for the distribution of components in hydrocarbon fluids because of the effect of the gravitational field. From 1940 to 1980, the petroleum industry was void of active research on compositional gradients but observations were reported.[4] By 1980, cubic EoS came into widespread use, enabling easy calculations of thermodynamic properties and Schulte was the first to solve the compositional gradients in reservoir fluids using an EoS.[29]

When a multi-component system is in true thermodynamic equilibrium in a gravity field, for each component in the system, the sum of the chemical potential and the gravitational potential should be constant. The condition of equilibrium is satisfied by the constraint 1.

$$\mu_i(P, X, T) = \mu_i(P^\circ, X^\circ, T) + M_i g(h - h^\circ) \quad (1)$$

For a N component system, the above condition represents N equations and, together with the constraint 2, the sum of mole fractions $X(h)$ must add to 1.

$$\sum_{i=1}^{N} X_i(h) = 1 \quad (2)$$

Composition $X(h)$ and pressure $P(h)$ can be solved simultaneously at any depth h. The thermodynamic equilibrium constraint 1 can be expressed in terms of fugacities of individual components in the system.

dx.doi.org/10.1021/ef201280d | Energy Fuels 2012, 26, 2548−2557

$$RT \ln\left(\frac{\hat{f}_i}{\hat{f}_i^{\circ}}\right) = M_i g(h - h^{\circ}) \text{ or}$$

$$\hat{f}_i = \hat{f}_i^{\circ} \exp\left(\frac{M_i g(h - h^{\circ})}{RT}\right) \quad (3)$$

Montel and Gouel solved eq 3 for an isothermal gravity chemical equilibrium (GCE), using an incremental oliostatic head instead of solving for pressure directly.[30] Thus, the procedure was only approximate because the compressibility effect of oil was not taken into consideration.

Whitson et al. in 1994 successfully solved the GCE problem, also taking into account the compressibility effect of oil.[31] The algorithm for this study is based in part on the Whitson procedure and solves the set of simultaneous nonlinear equations using a Newton−Raphson update for pressure and a Picard update for composition. The algorithm is solved in Microsoft Excel 2007, where the programming is in visual basic embedded in Excel Macros. PC-SAFT EoS is used for calculating the thermodynamic properties. Figure 4 represents the flowchart of the algorithm, and the description is provided in the subsequent paragraphs.

First, fugacities of the components f_i° at the reference depth h° are computed. Then, fugacities f_i at the new depth h are calculated from eq 3. This calculation needs to be made only once. Initial estimates of composition at depth h are simply the values at reference depth h°.

$$X_i^{(1)}(h) = X_i^{0} \quad (4)$$

For pressure, it is the reference pressure added with the column head pressure at reference depth density ρ°.

$$P^{(1)}(h) = P^{\circ}(h^{\circ}) + \rho^{\circ} g(h - h^{\circ}) \quad (5)$$

Now fugacities $f_i^{(n)}$ of the composition estimate $X^{(n)}$ at the pressure estimate $P^{(n)}$ are calculated. Corrected mole fractions are obtained using Picard's update.

$$Y_i^{(n)} = X_i^{(n)} \frac{\hat{f}_i(h)}{\hat{f}_i'^{(n)}(h)} \quad (6)$$

However, the sum of mole fractions should add to 1.

$$Q^{(n)} = 1 - \sum_{i=1}^{N} X_i^{(n)} \quad (7)$$

This error $Q^{(n)}$ is computed and used to update the pressure using a Newton−Raphson method

$$P^{(n+1)} = P^{(n)} + \frac{Q^{(n)}}{\left(\frac{\partial Q}{\partial P}\right)^n} \quad (8)$$

where

$$\left(\frac{\partial Q}{\partial P}\right)^n = \sum_{i=1}^{N} X_i \hat{f}_i \frac{\partial}{\partial P}\left(\frac{1}{\hat{f}_i'^{(n)}}\right) = -\sum_{i=1}^{N} \frac{X_i \hat{f}_i}{(\hat{f}_i'^{(n)})^2} \frac{\partial \hat{f}_i'^{(n)}}{\partial P} = -\sum_{i=1}^{N} Y_i^{(n)} \frac{\left(\frac{\partial \hat{f}_i'}{\partial P}\right)^n}{\hat{f}_i'^{(n)}} = -\sum_{i=1}^{N} Y_i^{(n)} \frac{\partial(\ln \hat{f}_i'^{(n)})}{\partial P} = -\sum_{i=1}^{N} Y_i^{(n)} \frac{\bar{V}_i^{(n)}}{RT} \quad (9)$$

It is interesting to observe that the derivative of error Q with respect to pressure can be written in terms of the mole fraction and partial molar volume of each component in the system. Thus, the updated pressure becomes

$$P^{(n+1)} = P^{(n)} - \frac{Q^{(n)}}{\sum_{i=1}^{N} Y_i^{(n)} \frac{\bar{V}_i^{(n)}}{RT}} \quad (10)$$

Convergence of solution is ensured using the following two tolerances:

$$|Q^{(n)}| < 10^{-12} \text{ and } \sum_{i=1}^{N} \left| \frac{\hat{f}_i}{\hat{f}_i'^{(n)}} - 1 \right| < 10^{-6} \quad (11)$$

Normalizing the values of $Y_i^{(n)}$ then yields the updated mole fractions $X_i^{(n+1)}$.

4. APPROXIMATE ANALYTICAL SOLUTION

Because of gravity, the reservoir fluid composition and properties vary with depth in a reservoir at thermodynamic equilibrium. Under a negligible temperature gradient, for each component in the system, the sum of chemical and gravity potentials should be constant. In comparison to the usual liquid−liquid equilibrium condition, which requires the chemical potential for each component to be equal in both phases, there is now an additional term because of the gravity field and the overall equilibrium can be expressed by

$$d\mu_i = M_i g \, dh \quad (12)$$

The difference in chemical potentials can be expressed in terms of fugacities of components in the system.

$$RT \ln\left(\frac{\hat{f}_i}{\hat{f}_i^{\circ}}\right) = M_i g \, dh \quad (13)$$

These fugacities can also be written in terms of fugacity coefficients, resulting in the expression 14.

$$RT \ln \frac{Z}{Z^{\circ}} + RT \ln \frac{\hat{\phi}_i}{\hat{\phi}_i^{\circ}} + RT \ln \frac{\rho_i}{\rho_i^{\circ}} = M_i g \, dh \quad (14)$$

dx.doi.org/10.1021/ef201280d | Energy Fuels 2012, 26, 2548−2557

In the limit of infinite dilution of asphaltene in oil, the partial molar volume of asphaltene can be considered independent of the concentration. Also, if the system is far away from its critical point, the partial molar volume can be assumed independent of pressure changes. Thus, the expression 14 becomes simplified as follows:[27]

$$RT \ln \frac{\rho^0}{\rho} + \overline{V}_i^{\infty}(P - P^o) + RT \ln \frac{\rho_i}{\rho_i^o} = M_i g \mathrm{dh} \quad (15)$$

Assuming negligible changes in the density of crude oils with depth, the pressure difference can be expressed in terms of head height and the resultant expression becomes

$$RT \ln \frac{\rho_i}{\rho_i^o} = [M_i g - \overline{V}_i^{\infty}\rho g](h - h^o) \text{ or}$$

$$\frac{\rho_i}{\rho_i^o} = \exp\left[\frac{(M_i - \overline{V}_i^{\infty}\rho)}{RT} g(h - h^o)\right] \quad (16)$$

A similar form of the above expression was first deduced by Muskat in 1930[27] but was applied to understand asphaltene compositional gradients only in 1988 by Hirschberg.[9] In the Hirschberg paper, the Huggins theory developed for a large linear molecule was applied for a bulky asphaltene molecule, resulting in the effective molar volume being significantly lower than the actual volume. Thus, expression 16 was never successfully used to determine the asphaltene gradient with depth. Using an accurate partial molar volume obtained from PC-SAFT, the successful implementation of this expression 16 to model the asphaltene compositional gradient is demonstrated in this work.

Mullins et al. derived and implemented an alternate asphaltene compositional gradient model using Flory–Huggins–Zuo (FHZ) solution theory, where the parameters are estimated by matching field measurements of the asphaltene gradient.[32] The parameters in our current work are estimated on the basis of asphaltene onset measurements in the laboratory, and all of the asphaltene compositional grading plots presented are pure predictions.

5. TAR-MAT FORMATION MECHANISM IN THE S FIELD

Tar mat is often close to geological discontinuities, including but not limited to oil–water contact (OWC). Tar mat is differentiated from heavy oil in that tar mat is characterized by high oil saturation associated with high residual oil saturation during logging.[33]

Tar mat can be caused by different processes, such as gas diffusion,[34] compositional grading,[35] biodegradation,[36] and flocculation of precipitated asphaltene.[37] A viable tar-mat formation mechanism can vary from field to field but must account for the following: (i) coeval nature of tar mat and oil leg, (ii) enrichment of asphaltene in tar mat, (iii) sharp compositional contrast with the overlying oil column, (iv) occurrence of tar mat in zones of higher horizontal permeability and higher porosity than the adjacent reservoir,[35] and (v) occurrence of tar mat at geological boundaries.

The reservoir considered for the tar-mat study is the S field from the Middle East. Samples from 27 cored wells were analyzed, and their organic content was assessed. Elemental analysis of tar mat and oil samples suggested a similar organic source for the tar mat and oil.[38] Tar-mat occurrence depth was estimated as ~9000 ft using rock evaluation, core density, and electric log approaches.[38]

The asphaltene compositional grading is the most feasible tar-mat formation mechanism for the S field based on the analysis summarized below: (i) The settling of precipitated asphaltene vertically through the oil column is not likely to lead to tar-mat formation because the reservoir pressure [4000 pounds per square inch absolute (psia)] is well above the AOP (2200 psia) needed to cause any asphaltene to precipitate. Injection of gas for enhanced oil recovery purposes did not cause any catastrophic asphaltene precipitation. Also, any small permeability contrasts are expected to lead to local micromat formation, and no such localized tat mats were detected.[39] (ii) Asphaltene can adsorb onto mineral surfaces[40] but is not a major route to the current tar-mat formation, because the tar mat is not ubiquitous within the reservoir.[41] (iii) The tar mat is located without any relation to the present day or paleo OWC.[38] Therefore, water washing does not play a role in the present tar-mat formation. Also, on the basis of laboratory experiments and numerical modeling, it is suggested that water washing alone is not a probable tar-mat formation mechanism.[42] (iv) Biomarker analysis showed no variation between the oil leg and tar mat.[38] Thus, the organic fluids are generated by the same source rock at the same maturity levels. This rules out any early charge of the structure by a low-mature asphaltene-rich fluid. (v) Biodegradation is capable of producing asphaltic oils by bacterial removal of *n*-alkanes. However, there were no signs of in-reservoir biodegradation, as observed from chromatograms.[41] The lack of biodegradation is in accordance with the reservoir temperature (120 °C), being higher than the maximum temperature compatible with bacterial activity (80 °C). (vi) Convective-related processes are not likely to be involved in tar-mat formation because the occurrence of large thermal convection in petroleum reservoirs is insignificant.[43] (vii) Oil cracking is negligible because the reservoir temperature (120 °C) is less than the minimum temperature required for thermal oil cracking (150 °C). (viii) Concluding evidence on tar-mat formation because of reservoir asphaltene destabilization caused by a late stage of gas charge is not available.[38,41] (ix) Movement of asphaltene in solution along gravitational field gradients is plausible, and the extreme cases of asphaltene compositional grading can lead to tar-mat formation.[9]

The asphaltene compositional grading introduced in this study is extended to further depths of the S field using PC-SAFT EoS to predict tar-mat formation.

6. RESULTS AND DISCUSSION

As observed from the expressions 1 and 12, the consideration of elevation difference produces the thermodynamic drive creating a composition gradient. Expression 16 is similar to the buoyancy term, where on the basis of the particle mass and system density, heavier components accumulate at the base and lighter components accumulate at the top of the column. For both the Tahiti and S fields considered in this work, negligible temperature gradient and equilibrium are assumed during the measurement of field data.

The molecular weight of saturates and A + R pseudo-components and aromaticity parameter can change with depth because individual components have individual degrees of compositional grading. However, the overall thermodynamic properties are predicted well by PC-SAFT even without considering such complex changes, as shown by the differential

liberation results.[44] Also, the highest compositional gradient will only be for asphaltene, which is separately considered as one of the components for the interest of this work.

6.1. Case I: Tahiti Field Consisting of Medium Oil. For reservoirs characterized by black and heavy oils, there has been uncertainty in ensuring flow communications, because the equilibrium distribution of fluid is characterized by only a small gradient of GOR. The largest gradient for these oils is often in the asphaltene. Thus, the idea of the asphaltene compositional gradient can be exploited to evaluate connectivity and other complexities in the reservoir.

The Tahiti field is offshore, in the Gulf of Mexico. It is a tilted reservoir with large horizontal (k_h = 600 mD) and vertical permeabilities ($k_v/k_h \sim 0.6$), enabling good convection. However, the reservoir is against a salt canopy and involves the risk of compartmentalization because of the faulting induced by salt buoyancy. Therefore, correct deduction of the connectivity of the reservoir is a key to decisions determining well placement for maximum economic production of the oil.

The successful working of the proposed PC-SAFT compositional grading algorithm is ensured by comparing the GOR variation prediction to the Tahiti field data. The results are shown in Figure 5. The reservoir has only a small GOR gradient, resulting in a small density change along the depth (3.4% over 3000 ft). The reservoir condition (~20 000 psia and 200 °F at 26 151 ft depth) ensures that the system is far away from the critical and bubble points.[19]

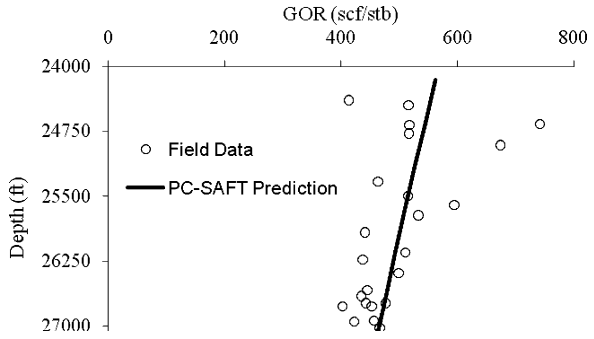

Figure 5. Variation of GOR with depth in the Tahiti field.

Figure 6 shows the PC-SAFT and approximate analytical solution predictions of the slopes of crude oil OD for the Tahiti field. The continuous lines are the predictions by PC-SAFT, and the broken lines are of analytical solution. A close match is observed between the predicted asphaltene concentration gradient and field data procured by DFA. The OD measurements were performed with an infrared wavelength of 1070 nm and directly infer the asphaltene content in the system.

From the PC-SAFT-generated asphaltene compositional grading curve, it is observed that the asphaltene content varies by a factor of 2 over 2500 ft vertically. All zones belong to the same reservoir, because the respective PC-SAFT asphaltene gradient curves have similar slope resulting from bulk crude oil properties. The north part of M21A has a much lower asphaltene concentration than the other parts of M21A. This implies that the north part of M21A is disconnected from the M21A central and south sands acknowledged by seismic and geochemistry data.[3] The M21A and M21B sands are the two primary reservoir sands. The M21B sand is in a different compartment than the M21A sands determined by formation pressure gradient and geochemistry fingerprinting of crude oil samples.[3] Thus, they are not in flow communication, and asphaltene compositional gradient analysis is consistent in this assessment.

The partial molar volume of asphaltene calculated by PC-SAFT is 1932 cm^3 with 0.1% variation over the range of depth considered (3000 ft). Thus, the average spherical diameter of an asphaltene particle is 1.83 nm and is in good agreement with the literature.[19] The crude oil A from the Tahiti field at downhole conditions also satisfies the assumptions of the analytical solution: (i) Observed from Figure 5, the Tahiti field has a low GOR gradient resulting in low crude oil density variations (3.4%) over the range of depth considered (3000 ft). (ii) The system is far away from the critical and bubble points. (iii) The asphaltene concentration is low enough (observed from Table 3) to assume the asphaltene partial molar volume to be independent of the species concentration.

For each of the zones, analytical solution is plotted together with field data and PC-SAFT-generated asphaltene compositional grading. The results are observed as broken lines in Figure 6, showing the excellent working of the simple analytical solution. Therefore, for any crude oil satisfying the above assumptions, the analytical solution can be used for an approximate estimate of the asphaltene compositional grading and sensitivity analysis of the gradient curves.

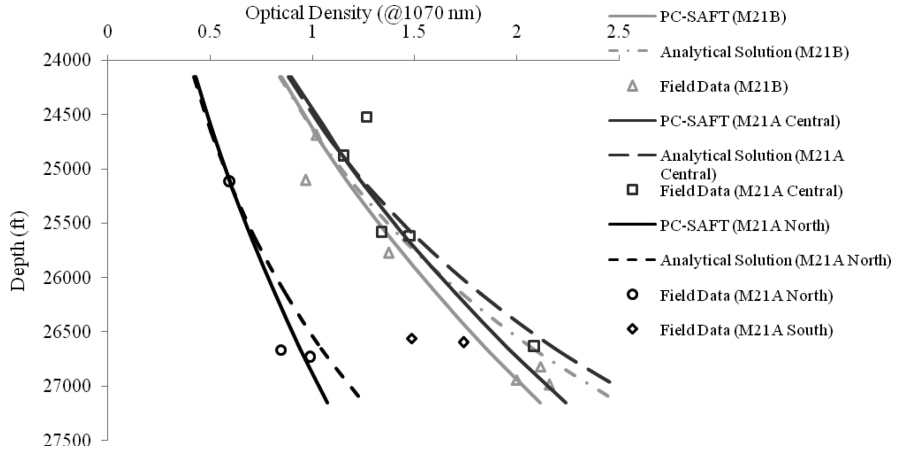

Figure 6. OD profile of crude oil (A) with depth in the Tahiti field.

dx.doi.org/10.1021/ef201280d | Energy Fuels 2012, 26, 2548–2557

In curve M21B, the reference depth was 24 687 ft. The deviation of analytical solution was only after ~25 500 ft and is accounted for compressibility effects when far away from the reference depth. In curves M21A central and north, the reference depths are 24 884 and 25 120 ft, respectively. There is a closer agreement of M21A north analytical solution with PC-SAFT-generated asphaltene compositional grading throughout the depth. The asphaltene partial molar volume and density of live oil inputted into the analytical solution are nearly the average of the system, giving better results over the depth considered.

6.2. Case II: S Field Consisting of Light Oil. Equilibrium distribution of high GOR fluids in a reservoir is characterized by a large gradient of GOR. The light crude oil considered here is from an onshore S field in the Middle East. The formation is mainly of carbonate rocks, with porosity ranging from 10 to 30%. The S field is a northeast−southwest elongated domal anticline structure, 16 miles long and 6 miles wide, with 160 km^2 of closure. The field is thought to result from pillows formed from movement of deeply buried Homruz salt. The faults are believed to have formed in response to salt piercement or compression forces because of the close proximity of the field to the orogenic zone.[39]

The S field is subdivided into an upper high-permeability layer (40−400 mD) and a lower low-permeability layer (10−15 mD). Production first commenced from the upper layer, which became flooded with water during the course of time, leaving a large amount of oil in the lower layer unproduced. Later on, several wells were drilled in this layer to produce the unproduced crude. Two of such wells are X and Y, respectively. Thus, understanding the connectivity of X and Y wells is important for the enhanced production of crude oil through flooding processes.

With the successful incorporation of asphaltene as one of the characterized crude B components at downhole conditions, a compositional grading algorithm is employed to predict the continuous properties of fluid. The dimensionless concentration of asphaltene is plotted in terms of dimensionless OD with the help of Beer−Lambert's law for low-concentration species, resulting in Figure 7. The normalization of the asphaltene concentration for the black line is with respect to well Y, and the normalization of the asphaltene concentration for the gray line is with respect to well Z.

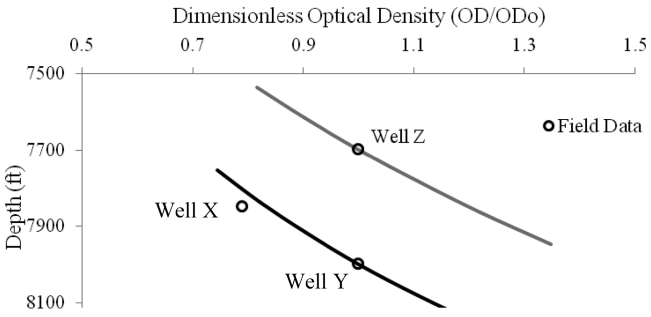

Figure 7. PC-SAFT-predicted asphaltene gradient in the S field.

The S field oil being light in nature produces a high asphaltene compositional grading on the order of 1.6 over 300 ft of depth. From the PC-SAFT asphaltene compositional grading, wells X and Y can have flow communication in the reservoir because they fall on the same gradient curve. The formation pressure of wells X and Y is ~4000 psia, and the formation pressure of well Z is 2854 psia. Thus, well Z is not in flow communication with wells X and Y, also corroborated by the PC-SAFT asphaltene compositional grading curve of well Y not passing through well Z. However, all wells belong to the same field because the slopes of corresponding asphaltene compositional gradient curves are similar, resulting from bulk crude oil properties.

The analytical solution cannot be applied for the S field because of high-density changes of 1.5% over the range of depth considered (450 ft). Also, the partial molar volume of asphaltene (average = 1460 cm^3) is dependent upon depth (variation of 1.3% for 450 ft depth).

6.3. Tar Mat in the S Field. A tar mat is in general associated with paraffinic oils, because a high degree of compositional grading and asphaltene precipitation problems are chiefly related to paraffinic oils. According to the most feasible tar-mat formation mechanism discussed above, the extreme manifestation of asphaltene compositional variation is the presence of a tar mat at the bottom of the field. Such a prediction of tar-mat occurrence depth, even though attempted by Hirshberg in 1988, could not be inferred from the *PVT* behavior of reservoir oil in the upper parts of the formation.[9]

The PC-SAFT asphaltene compositional grading, introduced in this study, is extended to further depths of the S field. After a depth of ~9000 ft, the asphaltene content suddenly increased to 5 mol %, as observed in Figure 8. This corresponds to an asphaltene weight percentage of 48 wt %, while measurements of the tar-mat samples report between 26 and 80 wt %.[41]

Above 9000 ft, asphaltene was stable in oil. Between 9000 and 9045 ft, the asphaltene concentration increased to an extent of phase separation. Thus, the tar mat formed is because of asphaltene precipitation as a result of compositional grading. The high and sudden contrast of the asphaltene content represents the transition from oil leg to a tar mat and is analogous to gas−oil contact depths in a reservoir. The PC-SAFT observed tar-mat formation is in accordance with the field observation of the tar-mat depth and the asphaltene content of the tar mat. Hence, this work successfully predicted the tar-mat occurrence depth from just knowing the pressure, temperature, and reservoir oil composition at a reference depth in the upper parts of the formation. Even under valid assumptions, tar mat cannot be predicted by the approximate analytical solution because it does not implicitly take into account the coexistence of another phase.

To conclude, the S field tar mat occurs because of transport of asphaltene in oil along chemical and gravitational potential gradients in the reservoir to the zone of asphaltene enrichment at the site of tar mat. The observed tar mat is located at the bottom of the reservoir and is characterized by a very low permeability, which increases the role of the permeability barrier already played by the dense limestone. This predictive model of tar-mat occurrence depth will be beneficial for field development and enhanced oil recovery procedures by a correct estimate of producible reserves and an effective placement of injection wells.

7. CONCLUSION

PC-SAFT is a highly useful EoS for modeling asphaltene. After the incorporation of asphaltene as one of the characterized crude oil components, isothermal asphaltene compositional grading was analyzed with the help of the successful algorithm presented in this paper. A simple analytical model based on solution thermodynamics is also presented under valid assumed

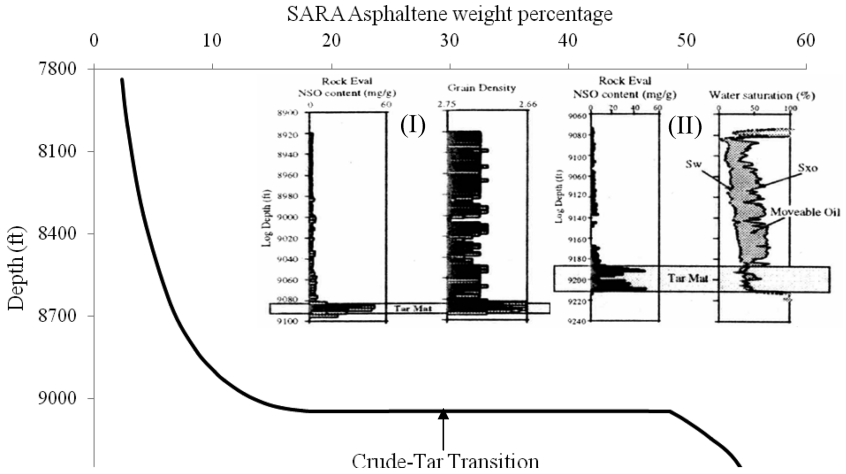

Figure 8. PC-SAFT prediction of tar mat in the S field. The insets (I and II) are well logs from two different wells identifying the tar mat in the S field.[38]

conditions. For both the medium and light oil reservoirs, PC-SAFT-generated asphaltene compositional grading showed a close agreement with the field data and evaluated the compartmentalization of the reservoirs. The analytical solution was successfully applied to predict the asphaltene compositional grading in the Tahiti reservoir. The results obtained in this work demonstrate that the proposed methods of PC-SAFT asphaltene grading and approximate analytical solution provide a useful tool to reduce the uncertainties related to reservoir compartmentalization and to optimize the logging during data acquisition.

The most feasible formation mechanism for the tar mat observed in the S field is identified as gravitational segregation. The PC-SAFT asphaltene compositional grading, introduced in the current study, is extended to further depths of the S field to model the tar-mat occurrence depth. This work successfully predicted the tar-mat occurrence depth from just knowing the pressure, temperature, and reservoir oil composition in the upper parts of the formation. The transition depth from oil leg to tar mat was sudden because of asphaltene phase separation and is analogous to gas−oil contact depths.

AUTHOR INFORMATION

Corresponding Author

*Telephone: 001-713-348-4900. E-mail: wgchap@rice.edu.

ACKNOWLEDGMENTS

This work was undertaken with the funding from the Oil R&D Subcommittee of the Abu Dhabi National Oil Company (ADNOC). The authors are thankful to Shahin Negahban, Dalia Abdullah, Sanjay Misra, and the Enhanced Oil Recovery Technical Committee for valuable support. The authors also thank Oliver Mullins, Jefferson Creek, George Hirasaki, Anju Kurup, Hariprasad Subramani, and Jianxin Wang for helpful discussions. A special thanks to Jan Hewitt for help in the preparation of this manuscript.

NOMENCLATURE

μ = chemical potential (Btu/mol)
P = system pressure (psia)
X = mole fraction
T = system temperature (°R)
M = molecular weight (lbm)
g = acceleration due to gravity (32.15 ft/s^2)
h = depth (ft)
R = universal gas constant (10.73 ft^3 psi °R^{-1} mol^{-1})
$\hat{f}$ = fugacity in mixture (psia)
ρ = density (lbm/ft^3)
Y = corrected mole fraction
Q = error
$\overline{V}$ = partial molar volume (ft^3/mol)
dh = difference in depths (ft)
Z = compressibility factor
$\hat{\phi}$ = fugacity coefficient in the system
$\Delta\rho$ = density difference between asphaltene and crude oil (lbm/ft^3)
ρ_i = molar density of component i (mol/ft^3)

Acronyms

GOR = gas/oil ratio
DFA = downhole fluid analysis
OD = optical density
EoS = equation of state
PC-SAFT = perturbed-chain statistical associating fluid theory
A + R = aromatics plus resins
STO = stock tank oil
SARA = saturates, aromatics, resins, and asphaltenes
PNA = polynuclear aromatic
MW = molecular weight
NIR = near infrared
AOP = asphaltene onset pressure
GCE = gravity chemical equilibrium
FHZ = Flory−Huggins−Zuo
OWC = oil−water contact

Superscripts

o = reference condition
N = number of components
n = iteration number

Subscripts

i = component number

REFERENCES

(1) Holt, T.; Lindeberg, E.; Ratkje, S. K. *SPE J.* **1983**, No. 11761.
(2) Betancourt, S. S.; Ventura, G. T.; Pomerantz, A. E.; Viloria, O.; Dubost, F. X.; Zuo, J. Y.; Monson, G.; Bustamante, D.; Purcell, J. M.;

Nelson, R. K.; Rodgers, R. P.; Reddy, C. M.; Marshall, A. G.; Mullins, O. C. *Energy Fuels* **2009**, *23*, 1178−1188.
(3) Mullins, O. C. *The Physics of Reservoir Fluids: Discovery through Downhole Fluid Analysis*; Schlumberger: Houston, TX, 2008.
(4) Espach, R. H.; Fry, J. *Trans. AIME* **1951**, *192*, 75−82.
(5) Panuganti, S. R; Punnapala, S.; Gonzalez, D. L.; Kurup, A.; Vargas, F. M.; Chapman W. G. *Proceedings of the SAFT Discussion Meeting*; Pau, France, Oct 24−25, 2011.
(6) Hoier, L.; Whitson, C. H. *SPE J.* **2001**, *4*, 525−535.
(7) Freed, D. E.; Mullins, O. C.; Zuo, J. Y. *Energy Fuels* **2010**, *24*, 3942−3949.
(8) Panuganti, S. R.; Vargas, F. M.; Kurup, A. S.; Chapman, W. G. *Proceedings of the Offshore Technology Conference*; Houston, TX, May 2−5, 2011.
(9) Hirschberg, A. *J. Pet. Technol.* **1988**, *40*, 89−94.
(10) Carpentier, B.; Arab, H.; Pluchery, E.; Chautru, J. M. *J. Pet. Sci. Eng.* **2007**, *58*, 472−490.
(11) Pittion, J. L. *Proceedings of the Organic Geochemistry Applied to Oil Exploration*; Rueil-Malmaison, France, Dec 12−15, 1983.
(12) Wilhelms, A.; Carpentier, B.; Huc, A. Y. *J. Pet. Sci. Eng.* **1994**, *12*, 147−155.
(13) Panuganti, S. R.; Vargas, F. M.; Gonzalez, D. L.; Kurup, A. S.; Chapman, W. G. *Fuel* **2011**, DOI: 10.1016/j.fuel.2011.09.028.
(14) Buckley, J. S.; Hirasaki, G. J.; Liu, Y.; Von Drasek, S.; Wang, J. X.; Gill, B. S. *Pet. Sci. Technol.* **1998**, *16*, 251−285.
(15) Gross, J.; Sadowski, G. *Ind. Eng. Chem. Res.* **2001**, *40*, 1244−1260.
(16) Gonzalez, D. L.; Hirasaki, G. J.; Chapman, W. G. *Energy Fuels* **2007**, *21*, 1231−1242.
(17) Spiecker, P. M.; Gawrys, K. L.; Kilpatrick, P. K. *J. Colloid Interface Sci.* **2003**, *267*, 178−193.
(18) Gonzalez, D. L.; David, T. P.; Hirasaki, G. J.; Chapman, W. G. *Energy Fuels* **2005**, *19*, 1230−1234.
(19) Zuo, J. Y.; Mullins, O. C.; Dong, C.; Dan, Z. *Nat. Resour.* **2010**, *1*, 19−27.
(20) Hirschberg, A.; Hermans, L. J. P. C. M. *Proceedings of the International Symposium on Characterization of Heavy Crude Oils and Petroleum Residues*; Lyon, France, June 25−27, 1984.
(21) Aske, N.; Kallevik, H.; Johnsen, E. E.; Johan, S. *Energy Fuels* **2002**, *16*, 1287−1295.
(22) Gonzalez, D. L. Ph.D. Thesis, Department of Chemical and Biomolecular Engineering, Rice University, Houston, TX, 2008.
(23) Gibbs, J. W. *Scientific Papers of J. Willard Gibbs: Thermodynamics*; Longmans, Green and Co.: New York, 1907.
(24) Gouy, L. G.; Chaperon, G. *Ann. Chim. Phys.* **1887**, *12*, 384.
(25) Duhem, P. *J. Phys. (Paris)* **1888**, *7*, 391.
(26) van der Waals, J. D. *Die Continuitat Des Gasformigen Und Flussigen Zustandes*; Kessinger Publishing: Whitefish, MT, 1900.
(27) Muskat, M. *Phys. Rev.* **1930**, *35*, 1384−1392.
(28) Sage, B. H.; Lacey, W. N. *Trans. AIME* **1939**, *132*, 120−131.
(29) Schulte, A. M. *Proceedings of the 55th Annual Technical Conference and Exhibition of Society of Petroleum Engineers (SPE) of American Institute of Mining, Metallurgical, and Petroleum Engineers (AIME)*; Dallas, TX, Sept 21−24, 1980.
(30) Montel, F.; Gouel, P. L. *Proceedings of the 60th Annual Technical Conference and Exhibition of Society of Petroleum Engineers (SPE)*; Las Vegas, NV, Sept 22−25, 1985.
(31) Whitson, C. H.; Trondheim, U.; Belery, P. *Proceedings of the Society of Petroleum Engineers (SPE) Centennial Petroleum Symposium*; Tulsa, OK, Aug 29−31, 1994; pp 443−459.
(32) Mullins, O. C. *Energy Fuels* **2010**, *24*, 2179−2207.
(33) Wilhelms, A.; Larter, S. R. *Mar. Pet. Geol.* **1994**, *11*, 418−441.
(34) Mullins, O. C.; Zuo, J. Y.; Freed, D.; Dong, C.; Reza, Z.; Elshahawi, H.; Pfeiffer, T.; Schechter, D.; Vance, H. *Proceedings of the Rio Oil and Gas Expo and Conference*; Rio de Janeiro, Brazil, Sept 13−16, 2010.
(35) Wilhelms, A.; Larter, S. R. *Geol. Soc. Spec. Publ.* **1995**, *86*, 87−101.
(36) Horsfield, B.; Heckers, J.; Leythaeuser, D.; Littke, R.; Mann, U. *Mar. Pet. Geol.* **1991**, *8*, 198−211.
(37) Zhang, M.; Zhang, J. *Chin. J. Geochem.* **1999**, *18*, 250−257.
(38) Carpentier, B.; Huc, A. Y.; Marquis, F.; Badr, A. E. R.; Al-Aldarous, A. A.; Al-Baker, S. *Proceedings of the Abu Dhabi International Petroleum Exhibition and Conference of Society of Petroleum Engineers (SPE)*; Abu Dhabi, United Arab Emirates, Nov 11−14, 1998.
(39) Abu Dhabi Company for Onshore Oil Operations (ADCO). *ADCO Proprietary Database*; ADCO: Abu Dhabi, United Arab Emirates, 2011.
(40) Crocker, M. E.; Marchin, L. M. *J. Pet. Technol.* **1988**, *40*, 470−474.
(41) Abu Dhabi Company for Onshore Oil Operations (ADCO). *ADCO Proprietary Report*; ADCO: Abu Dhabi, United Arab Emirates, Nov 2006.
(42) LaFargue, E.; Baker, C. *Am. Assoc. Pet. Geol.* **1988**, *72*, 263−276.
(43) England, W. A.; Mackenzie, A. S.; Mann, D. M.; Quigley, T. M. *J. Geol. Soc.* **1987**, *144*, 327−347.
(44) Panuganti, S. R.; Vargas, F. M.; Gonzalez D. L.; Chapman W. G. *Proceedings of the PetroPhase*; London, U.K., July 10−14, 2011.